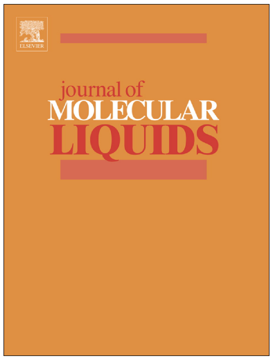

Pb(II) removal using carbon adsorbents prepared by hybrid heating system: Understanding the microwave heating by dielectric characterization and numerical simulation

Gabriela Durán-Jiménez, Virginia Hernández-Montoya, Jose Rodríguez Oyarzun, Miguel Ángel Montes-Morán, Eleanor Binner

PII:	S0167-7322(18)35359-5
DOI:	https://doi.org/10.1016/j.molliq.2018.12.143
Reference:	MOLLIQ 10219
To appear in:	*Journal of Molecular Liquids*
Received date:	16 October 2018
Revised date:	18 December 2018
Accepted date:	28 December 2018

Please cite this article as: Gabriela Durán-Jiménez, Virginia Hernández-Montoya, Jose Rodríguez Oyarzun, Miguel Ángel Montes-Morán, Eleanor Binner , Pb(II) removal using carbon adsorbents prepared by hybrid heating system: Understanding the microwave heating by dielectric characterization and numerical simulation. Molliq (2018), https://doi.org/10.1016/j.molliq.2018.12.143

Pb(II) removal using carbon adsorbents prepared by hybrid heating system: understanding the microwave heating by dielectric characterization and numerical simulation

Gabriela Durán-Jiménez[a*], Virginia Hernández-Montoya[b], Jose Rodríguez Oyarzun[a], Miguel Ángel Montes-Morán[c], Eleanor Binner[a]

[a]Microwave Process Engineering Research Group, Energy and Sustainability Research Division, Faculty of Engineering, University of Nottingham, University Park, Nottingham, NG7 2RD, United Kingdom
[b]TecNM/Instituto Tecnológico de Aguascalientes, Av. Adolfo López Mateos No. 1801 Ote. C.P. 20256, Aguascalientes, México.
[c]Instituto Nacional del Carbón, INCAR-CSIC, Apartado 73 E-33080, Oviedo, Spain

Abstract

This work studies the effect of microwaves in the synthesis of carbon adsorbents using pecan nutshell biomass as a precursor in a hybrid multimode microwave cavity avoiding the utilization of chemical activation or susceptors. The dielectric properties were calculated using the cavity perturbation method, and the power distribution of the electromagnetic field inside cavity was obtained by COMSOL Multiphysics. S-350-MW was obtained using at 350 °C and 200 W and it was characterized using elemental analysis, potentiometric titration, FT-IR and nitrogen adsorption isotherms at −196 °C. The adsorption of Pb(II), in single and binary solutions with Cu(II), Cd(II) and Zn(II) in batch systems indicate that the removal of Pb(II) is affected in the presence of Cu(II) due to the competition of these ions as a result of their similarities such as Pauling electronegativity. Finally, the removal of Pb(II) in continuous systems using packed bed columns showed the

---

[*]Corresponding author. Tel.: ++44 07727934248
E-mail address: gabriela.duranjimenez@nottingham.ac.uk, gaby_231105@yahoo.com.mx (Gabriela Durán-Jiménez)

pH has the most significant effect according to the variance analysis. The finding highlighted the importance of the acidic functional groups in the performance of carbonaceous adsorbents for the removal of Pb(II). Results of this study contribute to the understandings and application of a hybrid heating system and establish the basis of the role of heating processes in the preparation of carbonaceous adsorbents using microwaves. The Pb(II) removal efficiency achieved in this study is significantly higher than the values reported for carbons prepared by using microwave heating which employs susceptors and/or chemical agents reported in literature, demonstrating that it is possible to obtain effective carbon absorbents for the removal of Pb(II) without the use of any additional susceptors or chemical activation.

Keywords: Dielectric characterization, hybrid heating, lead removal, multicomponent systems, packed bed columns

1. Introduction

The water pollution caused by heavy metal ions is generated in metal processing operations, mining, rubber, plastic, leather and microelectronics processes. Their high toxicity, bio-accumulative behaviour, persistence in nature, and non-biodegradability highly threaten to living organisms [1-2]. Among all of the heavy metal ions, lead (Pb(II)) has been identified as one of the most toxic heavy metals because of its detrimental effects on the human nervous, blood circulation, kidneys, and reproductive system [3]. Various techniques such as chemical precipitation, membrane filtration, coagulation, ion-exchange, reverse osmosis and adsorption have been developed for the removal of Pb(II) from water.

Among the available methods, adsorption is a cost-effective, simple operation, reliable, and environmentally benign process for the removal of Pb(II) from water [4-5].

In recent years, the use of microwave heating to prepare carbonaceous adsorbent has attracted considerable attention as result of the claimed advantages compared with the use of conventional heating methods such as its volumetric nature, selectivity and fast heating, which could result in greater product uniformity, faster production rates and energy savings [6-11].

Biomasses such as date sphate, *Albizia lebbeck* seeds, oil palm shells, *macadamia* nut endocarp, coconut shells, oil-palm-stone, switchgrass, empty fruit bunch and larch wood have been used as precursors in the preparation of carbon adsorbents under microwave heating [12-17]. The procedures involve two-steps, including conventional carbonization at high temperatures (>600 °C) followed by the chemical activation using $FeCl_3$, KOH, $ZnCl_2$, $KMnO_4$, and H_3PO_4 under microwave radiation [8, 12, 18-21]. The principal concern related to the use of susceptors in microwave heating is the negation of any selective heating advantages of microwaves, as the sample load is conventionally heated by the susceptors. Additionally, the adopted methodology involves the pre-conditioning at high temperatures, which adds process steps and represents a real challenge in the processing time and costs.

In our previous work, Pb(II) was removed efficiently by carbonaceous adsorbents prepared by microwave without the utilisation of additional chemical agents or susceptors [22, 23]. It was demonstrated by the utilisation of a high electric field microwave system (single mode applicator) it is possible in one-step to obtain microporous carbonaceous adsorbents with basic nature and rich inorganic surface groups as calcium carbonate ($CaCO_3$) and calcium oxide (CaO) [23]. Additionally, it was found that using a hybrid heating cavity which combines conventional heating with microwaves it is possible to synthesize acid rich-oxygenated carbonaceous adsorbents, with functional groups such as carboxyl and carboxylic anhydrides [22]. Our results showed the performance of the carbonaceous adsorbents are directly correlated with the physiochemical properties which are critically influenced by the heating method and the system used in their preparation.

Despite of the big interest in applying microwave energy for preparation of carbonaceous adsorbents, most of the publications on preparation of carbon adsorbents have been studied using multimode cavities in modified-domestic microwaves [24-25]. This type of applicator results in a non-uniform electromagnetic field and multiple over heated locations [26-27], additionally, the dielectric properties of biomass, susceptors, chemical agents is not commonly reported. In this regard, through the assessment of the dielectric properties and the microwave heating behavior using computational simulations it is possible to predict the microwave-material interaction enabling the prediction non-desired reactions and improvements in system design.

In this work the preparation of carbonaceous adsorbents using pecan nutshell in a hybrid heating system and simulations using the Finite Element Method (FEM) by COMSOL Multiphysics® is reported for first time. Throughout dielectric characterization, the use of hybrid system was investigated as potential alternative to address the use of susceptors and chemical agents in the preparation of effective adsorbents. The applicability of the carbonaceous adsorbents was investigated in the removal of Pb(II) in multi-metal solutions (Pb-Cu, Pb-Cd, Pb-Zn) and in packed bed columns to predict its performance on industrial effluents.

2. Material and Methods

2.1 Carbonaceous adsorbents preparation

2.1.1 Raw material used as precursor of carbon

Pecan nutshells *(Carya illinoinensis)* were used as precursor of the carbonaceous materials. The precursor was obtained from an agro-food company in Aguascalientes, México, considering that México is one of the main producers of pecan nut, according to the Food and Agriculture Organization of the United Nations.

The pecan nutshells were milled and sieved to obtain a particle size of ~1 mm. They were then washed with deionized water at 25 °C until pH was constant and, finally, dried at 70 °C for 24 h.

2.1.2 Carbonaceous adsorbents

The preparation of the carbon adsorbent was carried out in a Carbolite MRF 16/22 hybrid system which include conventional and microwave heating. The nutshell was placed on alumina (99.9 % Al_2O_3) boat and the heating program comprised a heating ramp of 10 °C/min to 350 °C for 60 min, followed by microwave power of 200 W for 60 min (S-350-MW). An additional sample labeled S-350 was obtained using a heating ramp of 10 °C/min to 350 °C for 60 min but with no microwave heating.

2.2 Dielectric characterization and Multiphysics simulation

The dielectric properties of the sample, as well as mullite insulation of the cavity and alumina boat, were characterized using the cavity perturbation technique at 2450 MHz from 20 to 650 °C. The system comprised an electric tube furnace and a cylindrical copper TM_{0m0} resonant cavity connected to an HP 8753 vector network analyzer. 0.1 g of sample was packed with extra care in a quartz tube (3 mm ID) to obtain similar density ~0.76 g/cm^3 in each replication. The shift of resonant frequency and change of quality factor were measured allowing the determination of the dielectric constant and the dielectric loss factor [28]. All the samples were obtained by triplicated and averages are reported in Table 1.

To assess the sample behaviour inside of the cavity, electromagnetic and heat transfer co-simulations using COMSOL Multiphysics® were performed. A general sketch of the system and dimensions are presented in Fig. 1 and Table 2, respectively. Despite the rapid advances in the software tools, assumptions need to be made in order to simplify the system model and reduce the computational time. In the present work, simplifications of the model include not taking into account the molybdenum disilicide radiation elements inside the furnace (See Fig. 1), as these should induce negligible changes in the energy distribution and temperature profile [29], and also considering the sample as thermally insulated from the rest of the system. The simulations were performed at 2450 MHz and considering a base temperature of 350 °C, mimicking the temperature set by the electric heating of the cavity.

The system MRF 16/22 has no active tuning and no mode-stirring was used. In order to evaluate the adequate positioning of the sample, the sample boat position was simulated at different height from the bottom of the cavity. Positions for a range between 0 to 90 mm, in 5 mm steps were conducted to find the best position with regards to power coupling inside of the cavity. The system behaviour at the selected position was studied further using coupled electromagnetic and thermal simulation in order to evaluate the temperature evolution of the sample during microwave treatment.

2.3 Physicochemical characterization of carbonaceous adsorbents

The obtained carbonaceous adsorbents were characterized using different analytical techniques. The textural parameters were determined by nitrogen adsorption isotherms at -196 ºC using a Micromeritics ASAP 2420 apparatus. The elemental composition was obtained with a LECO CHNS-932 elemental analyzer and the oxygen content with a LECO VTF-900 equipment. The surface functional groups were identified by FT-IR spectroscopy using a Thermo Nicolet-6700 FT-IR spectrometer equipped with a deuterated triglycine sulfate detector (DTGS-KBr) to collect the IR spectra in the 4000‑500 cm^{-1} spectral range. The acidity was estimated by mixing 0.2 g of each carbon with 25 mL of 0.025 M NaOH in a closed flask and shaking for 24 h at 30 °C. Then the equilibrium solution was decanted, and the remaining concentration of NaOH was determined by potentiometric titration with 0.025 M HCl. The total basicity of each sample was obtained by a similar procedure, i.e., a solution of 0.025 M HCl was put in contact with the samples of carbon and the titration solution was 0.025 M NaOH. The point of zero charge was estimated following a previously reported methodology [30]. In this case, 0.120 g of each carbon was put in contact with 40 mL of 0.01 M NaCl at different initial pH values for 24 h. Initial pH values were adjusted by adding the appropriate amount of NaOH or HCl standards (0.1 M). The final pH was measured after 24 h under agitation at room temperature. The point of zero charge was determined as the pH value in a graph where the $pH_{final} = pH_{initial}$.

2.4 Adsorption of heavy metals

All metal ion solutions were prepared using distilled water and nitrate salts of the metals considered in this work ($Pb(NO_3)_2 \cdot 6H_2O$; $Cu(NO_3)_2 \cdot 3H_2O$; $Cd(NO_3)_2 \cdot 4H_2O$;

$Zn(NO_3)_2\cdot 6H_2O$). Analytical grade reagents from J.T. Baker and Sigma Aldrich Company were used.

2.4.1 Comparative study

To evaluate the performance of the carbonaceous adsorbents S-350 and S-350-MW in the removal of heavy metals from water, a comparative study was carried out in batch systems with a single metal solution. Four metal solutions with an initial concentration of 500 mg/L (e.g. Pb(II), Cu(II), Cd(II) and Zn(II)) were prepared by dissolving metal nitrate salts with deionized water. All the solutions were adjusted at initial pH 4 by adding nitric acid. A volume of 10 mL of metal solution was added to a plastic flask with 0.02 g of carbon after the flasks were placed in a shaking water bath at 30 °C and 150 rpm until the equilibrium was reached. Subsequently, the solution was separated from saturated adsorbent, and the equilibrium concentration was determined by their respective calibration curves, which were obtained by atomic absorption spectroscopy employing a Perkin Elmer Analyst 100 spectrometer. The contact time was selected based on preliminary kinetic experiments that demonstrated that the equilibrium time was established in the interval of 60-72 h. Therefore, the contact period was 72 h for all adsorption experiments.

Adsorption isotherms were performed using an initial metal concentration range from 50-1000 mg/L. The metal adsorption capacity (q, mg/g) of the samples S-350 and S-350-MW was calculated using a mass balance relationship given by Eq. (1).

$$q = \left(\frac{C_0 - C_e}{W}\right) V \tag{1}$$

where C_0 and C_e are the initial and equilibrium metal concentrations, respectively (mg/L), V is the volume of the solution (L), and W is the weight of the carbon used (g). All adsorption experiments were performed by triplicate with standard deviations below 5%. In this work an average value is presented.

2.4.2 Removal of heavy metals in binary systems

Adsorption experiments in a binary system were conducted in order to determine the competitive adsorption of Pb(II), Cu(II), Cd(II) and Zn(II) when a new divalent ion is present in the aqueous solution. An experimental design of the mixtures Pb–Cu, Pb–Cd and Pb–Zn was used to analyze the effect of the initial concentration of each component in the binary solution (See Table 3). The experiments were carried out in batch reactors using the sample denoted as S-350-MW, using experimental conditions: a mass-volume dosage of 2 g/L (carbon/metal solution), pH 4, 30 °C and agitation of 150 rpm for 72 h.

2.4.3 Removal of Pb(II)in continuous systems

Based on the results of the comparative study, the removal of Pb(II) on S-350-MW was performed in a dynamic system using a packed bed columns. For practical and large scale operations, a packed column allows the assessment of the required contact time and conditions to achieve the heavy metal removal in industrial applications. A packed column makes the best use of the concentration difference known to be the driving force for heavy metal adsorption. This leads for more efficient utilization of adsorbent capacity and also results in better quality of the effluent. In this study, a plastic column of 1.5 cm internal diameter and 4.5 cm of height was packed with 3.7 g of carbon S-350-MW and the efficiency of the carbon was investigated by varying relevant parameters as initial concentration, pH, temperature and flow rate. Table 4 shows the experimental design used for obtaining the breakthrough curves (L_9 orthogonal array of Taguchi method). Three levels of each parameter were analyzed using isothermal conditions (25, 30 and 35 °C) at initial concentration of Pb(II) of 50, 100 and 150 mg/L, initial pH solution of 3, 4 and 5 and flow rates of the solution through the column (Q) of 2, 3 and 4 mL/min. The response variable was the adsorbed amount of Pb(II) and the obtained data were analyzed statistically according to Taguchi methodology, with the purpose to identified the factors with more influence in the process [31].

Feed solutions were prepared with lead nitrate analytical grade and the deionized water. The solution was continuously pumped in the up-flow direction from the reservoir through the column, using a peristaltic pump. Effluent samples were taken at regular time intervals for determining the concentration of Pb(II) until the ratio of the equilibrium concentration regarding to the feed concentration ($C_t/C_0=0.9$) is reached.

Packed bed adsorption capacities were estimated via the numerical integration of the experimental breakthrough curves, Eq. 2:

$$q_e = \frac{Q}{M}\int_{t=0}^{t=t}\left(C_0 - C_t\right)dt \tag{2}$$

where q_e (mg/g) is the bed adsorption capacity for Pb(II) at tested experimental conditions, C_0, and C_t, (mg/L) are the Pb(II) concentrations in the feed and in the sample taken from the outlet of the column at time t (min), Q (mL/min) is the feed flow and M (g) is the mass of S-350-MW carbon packed in the column. The breakthrough point (t_b, min) was defined as the operating time of the adsorption column in which the concentrations ratio $C_t/C_0=0.1$ Likewise, the exhaustion point (t_e, min) was defined as the operating time of the adsorption column in which the concentrations ratio was 0.9 ($Ct/C_0=0.9$).

3. Results and discussion

3.1 Dielectric properties

The dielectric properties of S-350 and their temperature dependence are shown in Table 1. According to the chemical characterization, S-350 is a carbonized material obtained from nutshell and showed similar dielectric behavior to nutshell biomass [23]. The dielectric constant and loss factor exhibit significant changes with temperature, particularly at temperatures of above 550 °C where the remaining lignin in the sample starts to decompose to promote the formation of more ordered carbon, with the consequent sharp increase of dielectric properties related to the rise in electrical conductivity. These results are comparable to dielectric properties of biomass reported elsewhere [32].

3.2 Multiphysics simulations

The percentage of power coupled into the system as a function of the sample holder height is depicted in Fig.S1, which clearly highlights the importance of sample positioning. The simulation indicates the percent of power coupling varies from 39-99 %, with two distinct peaks at 25 and 60 mm, with coupling of 94.6 % and 99.3 % respectively. These results support the fact that sample positioning in multi-mode microwave systems is critical. Based on this, a 60 mm sample holder height was selected as suitable for performing microwave heating experiments in this system.

The power loss density is a measure of the microwave power converted into heat per unit volume and it is calculated using the Eq. 3

$$P_d = 2\pi f \varepsilon_0 \varepsilon'' E^2 \tag{3}$$

where P_d is the absorbed power of materials (W), f is the microwave frequency (Hz), ε_0 is the free space permittivity (8.854 ×10−12 F/m), and E is the electric field magnitude.

The electric field and the power loss density are shown in Fig. 2. Results showed a significant part of the microwave radiation is being absorbed by the insulation, due to a relatively small and low loss sample with a loss factor comparable to the insulation at 350 °C (mullite $\varepsilon_r = 1.89 - j0.0151$). It is important to note the preparation of the carbon was carried out in the same atmosphere where the sample was carbonized with no control of atmosphere. According to the results, future work includes the conventional treatment >550 °C in at inert atmosphere, as this would increase the microwave absorption in the sample as result of the increase of dielectric properties.

The temperatures attained within the sample bed during microwave heating cannot be measured, however it can be estimated by simulation. Fig. 3 shows the temperature increment after 60 min of microwave treatment. It was found the sample can reach a bulk temperature of around 400 °C and a maximum of around 430 °C (Fig. 3 a-b). The power loss density (Fig.3 a)) and temperature distribution (Fig. 3 b)) after 60 min of microwave treatment shows a clear hot-spot, and a relatively non-uniform heating pattern. This result can be expected in multimode cavities, however, after microwaves are off and according to the characterization analyses it is hypothesized that the temperature distribution was uniform as a result of heat conduction mechanisms throughout the sample volume.

3.3 Effect of microwave heating in the adsorption properties of carbon

Fig. 4 shows the effect of microwave heating in the adsorption of heavy metals. As can be seen in Fig. 4a, the adsorbed amount of Cu(II), Cd(II) and Zn(II) in the sample S-350-MW were similar to the sample S-350. More significant difference was observed in the removal of Pb(II), which amount increased from 187 to 200 mg/g for Pb(II) using the sample obtained by hybrid heating, S-350-MW, compared with S-350. This behavior can be associated with the increase of the specific surface area and total pore volume of S-350-MW (S_{BET} 30 m^2/g; V_T: 0.024) in comparison with the sample without microwave treatment, S-350 (S_{BET} 10 m^2/g; V_T: 0.0096). In this regard, it is important to note the specific surface area and total pore volume reported in the present work is low compared with activated carbons (>700 m^2/g) reported in literature because the carbonaceous sample obtained in this work was prepared without chemical activation these results are congruent with the data reported in [12]. The increment on the Pb(II) adsorption for the sample S-350-MW observed in Fig. 4, could be also attributed to the increment of oxygenated acidic groups (2.86 mmol/g) which was slightly higher than S-350 (2.55 mmol/g). These results are in agreement with the elemental composition, where the amount of oxygen was 45.14 % and 41.51 % for sample S-350-MW and S-350, respectively.

The FT-IR spectra are shown in Fig. 5. The principal signals can be assigned to the O-H stretching vibration of hydroxyl groups at 3428 cm^{-1} [33] and the peak at 1732 cm^{-1} is related to the C=O stretching vibration in carboxylic groups [34]. Also, other peaks are evident in the FT-IR spectra of all samples, which can be associated with the C=C stretching vibration (1605 cm^{-1}) and the bending out of the plane vibration of C-H bonds in aromatic structures (779 cm^{-1}) [35].

Based on the chemical characterization and the metal removal shown in Fig. 4, it is evident that the acidic functional groups of the carbon S-350-MW have a high affinity for Pb(II) in comparison with Cu(II), Cd(II) and Zn(II). This affinity can be associated with the chemical properties of each metal as covalent index, electronegativity and hydrated ionic radius of the metal ions. Specifically, the Pauling electronegativity is an important factor in determining which of the metals absorb with the highest preference. In this regard, the observed order of bonding preference was Pb(II) > Cu(II) > Cd(II) > Zn(II) and was in agreement with the Pauling electronegativity values (2.33> 1.9> 1.69 >1.60), respectively [36, 37]. Additionally, the results observed in Fig. 4 can be explained based on the strongest bond formed, which will be preferably formed with the metal with greatest covalent index. The covalent index for Pb(II), Cu(II), Cd(II) and Zn(II) are 7.18, 6.41, 5.51 and 4.54, respectively [38].

In this context, several authors have reported that the adsorbents with acidic surface group, preferentially adsorb soft ions such as Pb(II) and in the second place borderline ions such as Cu(II), Cd(II) and Zn(II) and finally, it would adsorb hard ions. Specifically, the binding properties of –COOH and –NH_2 groups from the 1:1 complex formation constants towards different metal ions have been reported [39]. It was reported in the binding groups containing a –COOH group, the degree of metal complexation was higher for Pb(II) > Cu(II) > Cd(II) >Zn(II). These results are congruent with the data reported in this work, where S-350-MW is a material with a high amount of oxygenated groups as carboxylic (-COOH) and phenolic (-OH) and the adsorption of heavy metals was preferentiality for Pb(II) > Cu(II) > Cd(II) >Zn(II) ions.

According to the results of Fig. 4a, the adsorption was higher for Pb(II), and in order to determine the maximum adsorption capacity of S-350 and S-350-MW, the adsorption isotherms of Pb(II) were studied (See Fig. 4b). The initial adsorption curve suggests that the adsorption occurs rapidly on the carbon surface at low concentrations for the two materials, however at higher initial concentration, a significant difference was observed for the sample S-350-MW and S-350, which the maximum adsorption capacity was 260 and

232 mg/g, respectively. The values reported in the present work are significantly higher than the values reported for carbons prepared in microwave heating with conventional carbonization and susceptors or chemical agents reported in literature, in which the maximum Pb(II) removal was 125 mg/g for a carbon obtained at 600 °C and activated using $FeCl_3$ and 640 W for 6 min (See Table 5). This results demonstrate that it is possible to obtain effective carbon absorbents for the removal of Pb(II) without the use of any additional susceptors or chemical activation.

3.4 Adsorption of Pb(II) in binary solutions

The adsorption of Pb(II) in binary systems were conducted using Cu(II), Cd(II) and Zn(II) as co-ions. The adsorption experiments were obtained at pH 4 and 30 °C according to the experimental design cited in Table 3. Particularly, the effect of metal concentration was studied in the range from 50 to 500 mg/L using at ratio of 1:1. The results are presented in Fig. 6 and it is clear that when the two metals coexisted in one solution, the competition between ions for the active sites takes place, decreasing the absorbed amount of the ion regarding to the achieved in single solution system (Fig. 6, black bars). Specifically, the adsorption of Pb(II) decreased significantly when the Cu(II) was used as co-ion as a result of the stronger competitive phenomena between the metals. The adsorption of Pb(II) was not affected significantly by the presence of Cd(II) or Zn(II). For example, the adsorption capacity of Pb(II) on the sample S-350-MW at initial concentrations of 500-500 mg/L of Pb(II)-Cu(II) was reduced from 213 to 51 mg/g (75 % less). However, the adsorption capacity of Pb(II) in presence of Cd(II) and Zn(II) decreased from 213 to 177 mg/g (16 %) and from 213 to 194 mg/g (9.14 %), respectively. This behavior can be associated with the differences and similarities between the metals, where

Pb(II) and the Cu(II) have a similar electronegativity. This finding highlights the importance of developing multicomponent adsorption systems to predict the performance of the adsorbents in industrial wastewaters.

3.5 Pb(II) breakthrough curves using packed bed columns

The batch method has been employed using single and multicomponent solutions for the removal of Pb(II), however, in order to evaluate the potential application of the adsorbents in industrial process, a study using packed bed columns is necessary. For the thermodynamic point of view, the mass transfer between the solid and the metal in solution determines their capability to be implemented in industrial process.

The comparison of the breakthrough curves of Pb(II) using S-350-MW is shown in Fig. 7. Design parameters of Pb(II) adsorption obtained from breakthrough curves are reported in Table 4. In this context, the breakthrough time (t_b) and the exhaustion time (t_e) were different in all the tests performed according to the experimental design (L_9 orthogonal array). The values are in the range from 7 to 610 min for t_b and from 3,610 to 13,737 for t_e. A general behavior was observed and at low feed concentration of Pb(II) (50 mg/L), the exhausting time was higher (13,330), while a high feed concentration of Pb(II) (150 mg/L) the exhausting time, t_e, was 3,610 min. This behavior could be explained by the lower concentration gradient caused a slower transport mass. The Fig. 7 and Table 4 shows that at a higher flow rate (4 mL/min), the breakthrough point, t_b, is reached on the first minutes of operation (7 min) (see C-3, C-4 and C-8). As a result, at a low flow rate, the residence time increased, allowing the Pb(II) ions to diffuse and interact with the active surface groups in the adsorbent. The performance of each breakthrough curves was characterized by estimation of the mass transfer zone (MTZ). In Table 4 are reported MTZ values, and it is evident that the MTZ increase with the feed flow rate while Δt decreased with an increment in pH. According to literature, the most important parameter affecting the metal uptake is the pH of adsorption medium. The initial pH of solution determines the adsorption mechanisms and reflects the nature of the physicochemical interactions between the metallic species in solution and the adsorbent. This behavior was observed in the present work because according to the statistical analysis presented in Table 6, the factor with more influence in the adsorption process in the dynamic system was the pH followed by the feed concentration, flow rate and finally, the temperature. Specifically, the variance for these factors was 34.4, 5.45, 0.47 and 0.18, respectively (See Table 6). In this context, it is well known that the pH of the solution affects the surface charge of the adsorbent, the degree of ionization, and the speciation of the surface functional groups. Particularly, the sample S-350-MW has a point of zero charge (PH_{PZC}) of 3.6 and has an acidic character. The increase in metal removal with the pH can be explained on the basis of at higher pH, decrease the competition between proton (H^+) and metal cation (Pb(II)) and the surface charge of material is negative, favoring the adsorption of cationic species as the heavy metals.

The maximum Pb(II) uptake of packed bed column is 282 mg/g using an initial concentration of 100 mg/L, pH 5, 25 °C and a flow rate of 3 mL/min. This value is comparable with the data obtained in batch system (260 mg/g). Consequently, these results suggest that the dynamic adsorption process in bed packed columns are not affected by mass transfer process and the results are in agreement with the low specific surface and porosity of S-350-MW.

In summary, the results show that the carbon S-350-MW can be successfully employed for the removal of Pb(II) and based on breakthrough curve data, the suggested conditions for higher Pb(II) removal are at feed concentration of 150 mg/L, pH 5 and feed flow 3 mL/min.

4. Conclusions

The results obtained in this work indicate that it is possible to obtain efficient carbonaceous adsorbents for the removal of Pb(II) and other heavy metals in single, multi-component and in packed bed columns using a hybrid heating system at comparatively low temperatures and low microwave power and without the utilization of any additional susceptors or chemical activation. Particularly, Multiphysics simulations showed by using a power of 200 W, it is possible to increase the sample temperature (by 50 °C). Experimentally, it was found that the addition of a microwave heating step promoted the formation of acidic functional groups in the surface of the carbon, which lead to a higher metal adsorption. The results show that hybrid heating systems can be fruitfully employed for the preparation of carbon adsorbents for the removal of Pb(II) from wastewater in single as well as in multi-component systems. Besides the low porosity, the chemical functionalities play the determining role in the effective metal uptake in dynamic systems, which allowed a better performance than activated carbon reported in literature. Additionally, the results provide the basis for the suitable design of microwave reactors to address the challenges involved in the treatment of microwave-transparent samples in multimode cavities. The use of retort furnaces can allow hybrid heating with a tight atmospheric control as well as, possibly, highly efficient microwave treatment.

Acknowledgements

This work was supported by CONACyT under the grant (389535)

References

[1] B. Hayati, A. Maleki, F. Najafi, H. Daraei, F. Gharibi, G. McKayc, Super high removal capacities of heavy metals (Pb2+ and Cu2+) using CNT dendrimer, J Hazard Mater, 336 (2017) 146–157.

[2] F. Wang, Y. Pan Y., P. Cai, T. Guo, X. Huining, Single and binary adsorption of heavy metal ions from aqueous solutions using sugarcane cellulose-based adsorbent, Bioresource Technol, 241 (2017) 482–490.

[3] B. Xiang, D. Ling, H. Lou, H. Gu, 3D hierarchical flower-like nickel ferrite/manganese dioxide toward lead (II) removal from aqueous water, J Hazard Mater, 325 (2017) 178–188.

[4] Z.A. Alothman, Y.E. Unsal, M. Habila, M. Tuzen, M. Soylak, A membrane filtration procedure for the enrichment separation, and flame atomic absorption spectrometric determinations of some metals in water, hair, urine, and fish samples, Desalin Water Treat, 53 (2014) 3457–3465.

[5] Y. Lei, J.-J. Guan, W. Chen, Q.-F. Ke, C.-Q. Zhang, Y.-P. Guo, Fabrication of hydroxyapatite/chitosan porous materials for Pb (II) removal from aqueous solution, RSC Adv, 5 (2015) 25462–25470.

[6] M. Tripathi, J.N. Sahu, P. Ganesan, T.K. Dey, Effect of temperature on dielectric properties and penetration depth of oil palm shell (OPS) and OPS char synthesized by microwave pyrolysis of OPS, Fuel, 153 (2015) 257–266.

[7] F. Mechati, C. Bouchelta, M. S. Medjram, R. Benrabaa, N. Ammouchi, Effect of hard and soft structure of different biomasses on the porosity development of activated carbon prepared under N_2/microwave radiations, J Environ Chem Eng, 3 (2015) 1928–1938.

[8] Z. Zhang, X. Wang, Y. Wang, S. Xia, L. Chen, Y. Zhang, J. Zhao, Pb(II) removal from water using Fe-coated bamboo charcoal with the assistance of microwaves, J Environ Sci, 25(5) (2013) 1044‑1053.

[9] Z. Emami, S. Azizian, Preparation of activated carbon from date sphate using microwave irradiation and investigation of its capability for removal of dye pollutant from aqueous media, J Anal Appl Pyrol, 108 (2014) 176‑184.

[10] M.J. Ahmeda, S. K. Theydan, Optimization of microwave preparation conditions for activated carbon from Albizia lebbeck seed pods for methylene blue dye adsorption, J Anal Appl Pyrol, 105 (2014) 199–208.

[11] R. H. Hesas, A. Arami-Niya, W. M. A. W. Daud, J.N. Sahu, Comparison of oil palm shell-based activated carbons produced by microwave and conventional heating methods using zinc chloride activation, J Anal Appl Pyrol, 104 (2013) 176-184.

[12] Y. Wang, X. Wang, X. Wang, M. Liu, L. Yang, Z. Wu, S. Xia, J. Zhao, Adsorption of Pb(II) in aqueous solutions by bamboo charcoal modified with $KMnO_4$ via microwave irradiation, Colloids Surf A, 414 (2012) 1‑8.

[13] O. Pezoti Junior, A. L. Cazetta, R. C. Gomes, E. O. Barizão, I. P.A.F. Souza, A. C. Martins, T. Asefa, V. C. Almeida, Synthesis of $ZnCl_2$-activated carbon from macadamia nut endocarp (Macadamia integrifolia) by microwave-assisted pyrolysis:

Optimization using RSM and methylene blue adsorption, J Anal Appl Pyrol, 105 (2014) 166‑176.

[14] J. Guo, A.C. Lua, Preparation of activated carbons from oil-palm-stone chars by microwave-induced carbon dioxide activation, Carbon, 38 (2000) 1985–1993.

[15] R. Zhou, H. Lei, J.L. Julson, Effects of reaction temperature, time and particle size on switchgrass microwave pyrolysis and reaction kinetics, Int J Agric & Biol Eng, 6(1) (2013) 53-61.

[16] R. Omar, A. Idris, R. Yunus, K. Khalid, M.I. Aida Isma, Characterization of empty fruit bunch for microwave-assisted pyrolysis, Fuel, 90 (2011) 1536–1544.

[17] M. Miura, H. Kaga, A. Sakurai, T. Kakuchi , K. Takahashi, Rapid pyrolysis of wood block by microwave heating, J Anal Appl Pyrol, 71 (2004) 187–199.

[18] M.W. Yap, N.M. Mubarak, J.N., Sahu, E.C. Abdullah, Microwave induced synthesis of magnetic biochar from agricultural biomass for removal of lead and cadmium from wastewater, J Ind Eng Chem, 45 (2017) 287–295.

[19] T. M Alslaibi, I. Abustan, M. Ahmad, A. Foul, Comparison of Activated Carbon Prepared from Olive Stones by Microwave and Conventional Heating for Iron (II), Lead (II), and Copper (II) Removal from Synthetic Wastewater, Environ Prog Sustain, 33(4) 2014, 1074-1085.

[20] S. Yao, J. Zhang, D. Shen, R. Xiao, S. Gu, M. Zhao, J. Liang, Removal of Pb(II) from water by the activated carbon modified by nitric acid under microwave heating, J Colloid Interf Sci, 463 (2016) 118–127.

[21] Q.H. Lin, H. Cheng, G.Y. Chen, Preparation and characterization of carbonaceous adsorbents from sewage sludge using a pilot-scale microwave heating equipment, J Anal Appl Pyrol, 93 (2012), pp. 113-119.

[22] G. Durán-Jiménez, V. Hernández-Montoya, M.A. Montes-Morán, M. Teutli-León, New oxygenated carbonaceous adsorbents prepared by combined radiant/microwave heating for the removal of Pb^{2+} in aqueous solution, J Anal Appl Pyrol, 113 (2015) 599–605.

[23] G. Duran Jimenez, T. Monti, J.J. Titman, V. Hernandez-Montoya, S.W. Kingman, E.R. Binner, New insights into microwave pyrolysis of biomass: Preparation of carbon-based products from pecan nutshells and their application in wastewater treatment, J Anal Appl Pyrol, 124 (2017) 113–121.

[24] K. Pitchai, S.L. Birla, J. Subbiah, D. Jones, H. Thippareddi, Coupled electromagnetic and heat transfer model for microwave heating in domestic ovens, J Food Eng, 112 (2012) 100-111.

[25] G. Brodie, The influence of load geometry on temperature distribution during microwave heating, Trans Asabe, 51 (2008) 1401-1413.

[26] H. H. Sait, A. A. Salema, Microwave dielectric characterization of Saudi Arabian date palm biomass during pyrolysis and at industrial frequencies, Fuel, 161 (2015) 239‑247.

[27] D.A. Jones, T.P. Lelyveld, S.D. Mavrofidis, S.W. Kingman, N.J. Miles, Microwave heating applications in environmental engineering-a review, Resour Conserv and Recy, 34 (2002) 75–90.

[28] A. Smith, E. Lester, K. Thurecht, S. Kingman, J. Harfi, G. Dimitrakis, J. Robinson, D. Irvine, Temperature Dependence of the Dielectric Properties of 2,2′-Azobis(2-methyl-butyronitrile) (AMBN), Ind Eng Chem Res, 49 (2010) 3011–3014.

[29] J. Binner, B. Vaidhyanathan, J. Wang, D. Price, M. Reading, Evidence for Non-Thermal Microwave Effects Using Single and Multimode Hybrid Conventional/Microwave Systems, International Microwave Power Institute 42(2), (2008) 47-63.

[30] P.C. Faria, J.J. Orfa, M.F. Pereira, Adsorption of anionic and cationic dyes on activated carbons with different surface chemistries, Water Res, 28 (2004) 2043‑2052.

[31] G. Durán-Jiménez, V. Hernández-Montoya M.A. Montes-Morán, A. Bonilla-Petriciolet, N.A. Rangel-VázquezAdsorption of dyes with different molecular properties on activated carbons prepared from lignocellulosic wastes by Taguchi method, Micropor Mesopor Mat, 199 (2014)99-107.

[32] A.A. Salema, F.N. Ani, J. Mouris, R. Hutcheon, Microwave dielectric properties of Malaysian palm oil and agricultural industrial biomass and biochar during pyrolysis process, Fuel Process Technol,166 (2017) 164–173.

[33] J.C.P. Vaghetti, E.C. Lima, B. Royer, B.M. da Cunha, N.F. Cardoso, J.L. Brasil, S.L.P. Dias, Pecan nutshell as biosorbent to remove Cu(II), Mn(II) and Pb(II) from aqueous solutions, J Hazard Mater,162 (2009) 270‑280.

[34] Y. Guo, D.A. Rockstraw, Physical and chemical properties of carbons synthesized from xylan, cellulose, and Kraft lignin by H_3PO_4 activation, Carbon, 44 (2006) 1464‑1475.

[35] O. M˘asek, V. Budarin, M. Gronnow, K. Crombie, P. Brownsort, E. Fitzpatrick, P. Hurst, Microwave and slow pyrolysis biochar-comparison of physical and functional properties, J Anal Appl Pyrolysis, 100 (2013) 41‑48.

[36] C. R. Teixeira Tarley, M. A. Zezzi Arruda, Biosorption of heavy metals using rice milling by-products. Characterisation and application for removal of metals from aqueous effluents, Chemosphere, 54 (2004) 987–995.

[37] R. Balasubramanian, S. V. Perumal, K. Vijayaraghavan, Equilibrium Isotherm Studies for the Multicomponent Adsorption of Lead, Zinc, and Cadmium onto Indonesian Peat, Ind Eng Chem Res, 48 (2009) 2093–2099.

[38] E. Nieboer, W.A.E. Mcbryd, Free-energy Relationships in Coordination Chemistry. 111. A Comprehensive Index to Complex Stability, Can J Chem, 51 (1973) 2512-2524.

[39] V. M. Nurchi, G. Crisponi, I. Villaescusa, Chemical equilibria in wastewaters during toxic metal ion removal by agricultural biomass, Coordin Chem Rev, 254 (2010) 2181-2192.

Captions

Fig. 1 Schematic representation of the hybrid heating system MRF 16/22

Fig. 2 Electric field distribution (V/m) (a) and Electromagnetic power loss density (W/m^3) (b) within the cavity.

Fig. 3 Electromagnetic power loss density (W/m^3) (a) and temperature distribution of the sample after 60 minute microwave heating (b).

Fig. 4 Adsorption of heavy metals on the samples S-350 and S-350-MW (a) and adsorption isotherms of Pb (II) (b). Experimental conditions: pH=4, T=30°C, agitation: 150 rpm, mass to volume ratio: 2 g/L, initial concentration: (500 mg/L for (a) and 50-1000 mg/L for (b)). Ceq represent the equilibrium concentration

Fig. 5 FT-IR spectra of the adsorbent S-350 (dotted line) and S-350-MW (continuous line)

Fig. 6 Adsorption capacities of heavy metals from binary mixtures on S-350-MW. Experimental conditions: pH=4, T=30°C, agitation: 150 rpm, mass to volume ratio: 2 g/L, initial concentration: 50-500 mg/L

Fig. 7 Breakthrough curves adsorption of Pb(II) in aqueous solution using packed bed columns at different experimental conditions (cited in Table 4)

Table 1. Dielectric properties dependence with temperature of S-340

T(°C)	2470 MHz	
	Dielectric constant, ε'	Loss factor, ε''
20	2.39± 0.02	0.070± 0.00
50	2.39± 0.01	0.069± 0.00
100	2.40± 0.04	0.063± 0.00
150	2.18± 0.00	0.041± 0.00
200	2.10± 0.05	0.022± 0.00
250	2.06± 0.08	0.015± 0.00
300	2.14± 0.08	0.014± 0.00
350	2.13± 0.07	0.012± 0.00
400	2.14± 0.03	0.011± 0.00
450	2.15± 0.08	0.015± 0.00
500	2.16± 0.09	0.043± 0.00
550	2.23± 0.11	0.156± 0.00
600	2.52± 0.10	0.678± 0.00
650	5.09± 0.20	2.400± 0.20

Table 2. Dimension of the hybrid multimode cavity and components

Geometry	Width - x (mm)	Depth - y (mm)	Height - z (mm)
Inner chamber (block)	300	300	288
Outer chamber (block)	400	360	388
Waveguide (block) WR340	86.3	122.3	43.2
Holder (elliptical cylinder)	27	137	60
Sample (elliptical cylinder)	24	120	2

Table 3. Experimental design used in the adsorption of heavy metals in binary systems

Concentration of metal *i* (mg/L)	Concentration of metal *j* (mg/L)			
	50	100	250	500
50	50, 50	50, 100	50, 250	50, 500
100	100, 50	100, 100	100, 250	100, 500
250	250, 50	250, 100	250, 250	250, 500
500	500, 50	500, 100	500, 250	500, 500

i=Pb^{2+} j=Cu^{2+}, Cd^{2+}, Zn^{2+}

i

Table 4. Experimental design used in the continuous adsorption experiments (L_9 orthogonal array of Taguchi method), design parameters and adsorption results.

Experiment	Factor				Breakthrough parameters				
	A: C_0 (mg/L)	B: pH	C: T (°C)	D: Q (mL/min)	t_b (min)	t_e (min)	Δt (min)	MTZ (cm)	$_e^*$ (mg/g)
C-1	50	3	25	2	250	10075	9825	4.39	100
C-2	50	4	30	3	157	13330	13173	4.45	204
C-3	50	5	35	4	212	11200	10988	4.41	209
C-4	100	3	30	4	7	5917	5910	4.49	130
C-5	100	4	35	2	610	11312	10702	4.26	245
C-6	100	5	25	3	200	8614	8414	4.40	282
C-7	150	3	35	3	50	3610	3560	4.44	145
C-8	150	4	25	4	40	6120	6080	4.47	279
C-9	150	5	30	2	190	8029	7839	4.39	255

[*] Obtained by numerical integration

Table 5. Comparison of the maximum adsorption capacity of Pb(II) by different carbonaceous adsorbents reported in literature

Biomass	Conventional heating	Agent/susceptor	Microwave treatment	Pb(II) removal (mg/g)	Reference
Pecan nutshell	350	-	200 W, 60 min	260	This study
Coconut shell	-	$FeCl_3$	800 W, 20 min	100	18
Olive stones	600	KOH	565, 7 min	23.4	19
Rice husk	600	$ZnCl_2$	800 W, 15 min	143	20
Bamboo	600	$KMnO_4$	640 W, 6 min	55	12
Bamboo	600	$FeCl_3$	640 W, 6	125	8
Pine wood	600	$ZnCl_2$	8000 W, 106	43	21
Sewage sludge	600	H_3PO_4	8000 W, 103	55	21
Sewage sludge	600	KOH	8000 W, 107	50	21

Table 6. Response for the Taguchi analysis and analysis of variance of the Pb(II) removal in continuous systems using packed bed columns.

Factor	Mean $(S/N)_{HB}$			Analysis of variance		
	Level 1	Level 2	Level 3	Degrees of freedom	Sum of squares	Variance
A	44.25	46.35	46.75	2	10.90	5.45
B	41.88	47.63	47.85	2	68.81	34.40
C	46.02	45.53	45.80	2	0.36	0.18
D	45.36	46.14	45.86	2	0.95	0.47
Error						
Total				8	81	

Highlights

►Hybrid heating process that combine microwave and conventional heating was used for the preparation of adsorbents ► Dielectric properties and numerical simulation were used to estimate the effect of microwave ►Carbons were obtained in one step without any susceptors ► Single, multicomponent and packed bed columns were used for the removal of Pb(II) from water

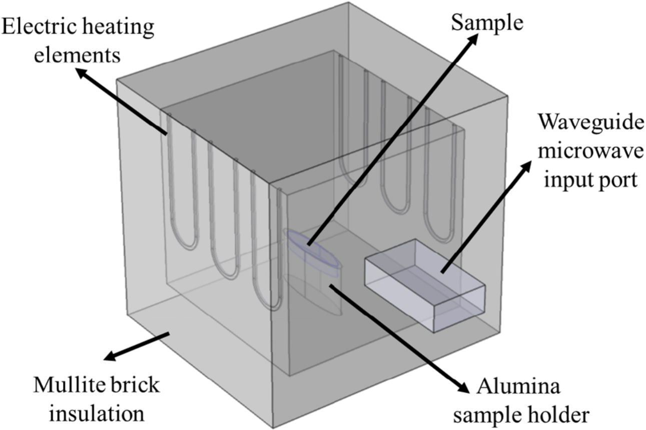
Electric heating elements
Sample
Waveguide microwave input port
Mullite brick insulation
Alumina sample holder

Figure 1

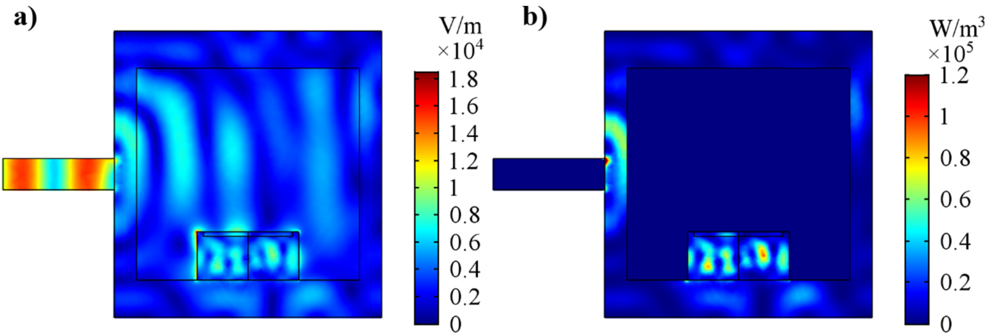

Figure 2

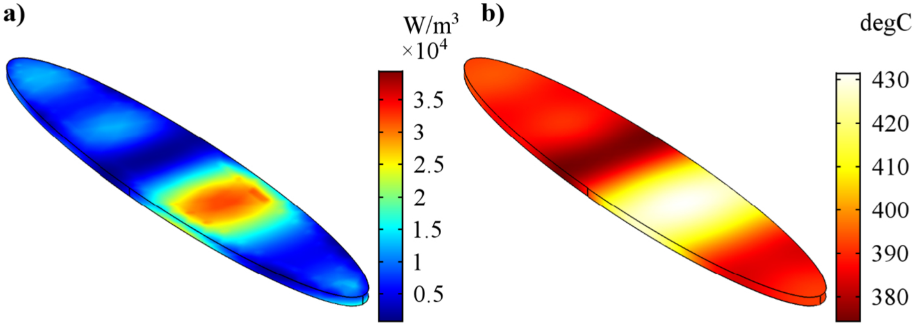

Figure 3

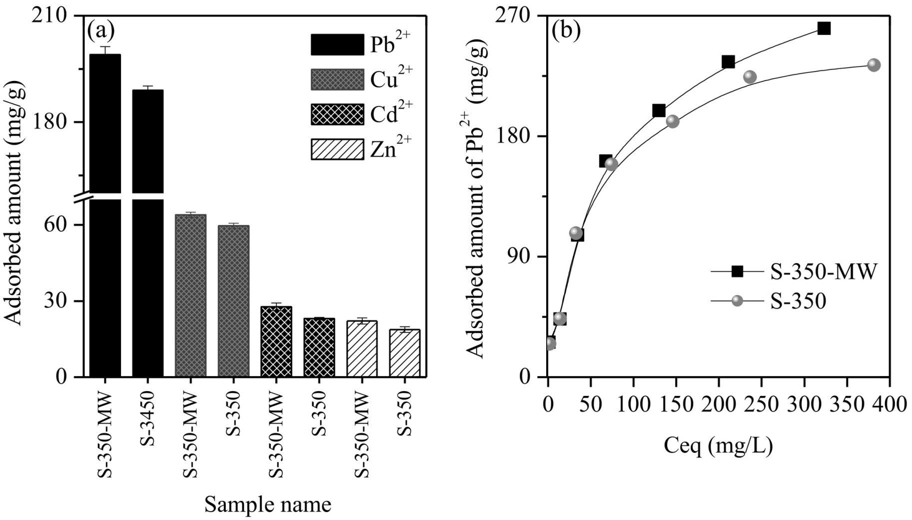
(a)
Adsorbed amount (mg/g)
210
180
60
30
0
Pb^{2+}
Cu^{2+}
Cd^{2+}
Zn^{2+}
S-350-MW
S-3450
S-350-MW
S-350
S-350-MW
S-350
S-350-MW
S-350
Sample name
(b)
Adsorbed amount of Pb^{2+} (mg/g)
270
180
90
0
0
50
100
150
200
250
300
350
400
Ceq (mg/L)
S-350-MW
S-350

Figure 4

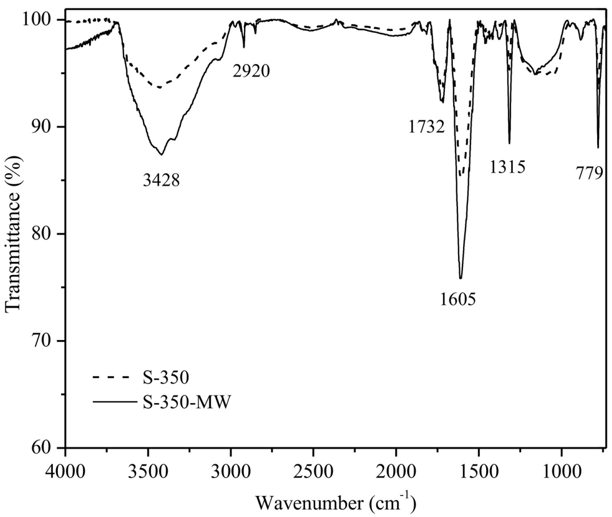

Transmittance (%)
100
90
80
70
60
4000
3500
3000
2500
2000
1500
1000
Wavenumber (cm^{-1})
3428
2920
1732
1605
1315
779
S-350
S-350-MW

Figure 5

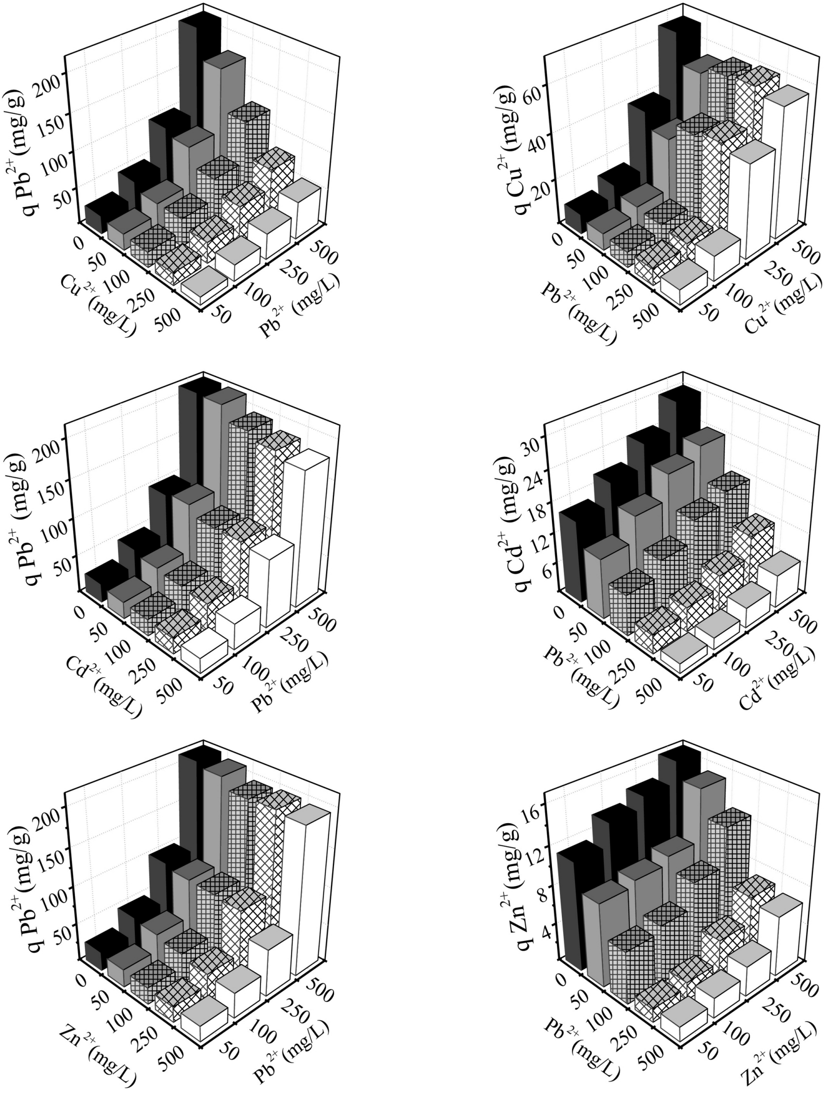
q Pb^{2+} (mg/g)
50
100
150
200
0
50
100
250
500
Cu^{2+} (mg/L)
50
100
250
500
Pb^{2+} (mg/L)
q Cu^{2+} (mg/g)
20
40
60
0
50
100
250
500
Pb^{2+} (mg/L)
50
100
250
500
Cu^{2+} (mg/L)
q Pb^{2+} (mg/g)
50
100
150
200
0
50
100
250
500
Cd^{2+} (mg/L)
50
100
250
500
Pb^{2+} (mg/L)
q Cd^{2+} (mg/g)
6
12
18
24
30
0
50
100
250
500
Pb^{2+} (mg/L)
50
100
250
500
Cd^{2+} (mg/L)
q Pb^{2+} (mg/g)
50
100
150
200
0
50
100
250
500
Zn^{2+} (mg/L)
50
100
250
500
Pb^{2+} (mg/L)
q Zn^{2+} (mg/g)
4
8
12
16
0
50
100
250
500
Pb^{2+} (mg/L)
50
100
250
500
Zn^{2+} (mg/L)

Figure 6

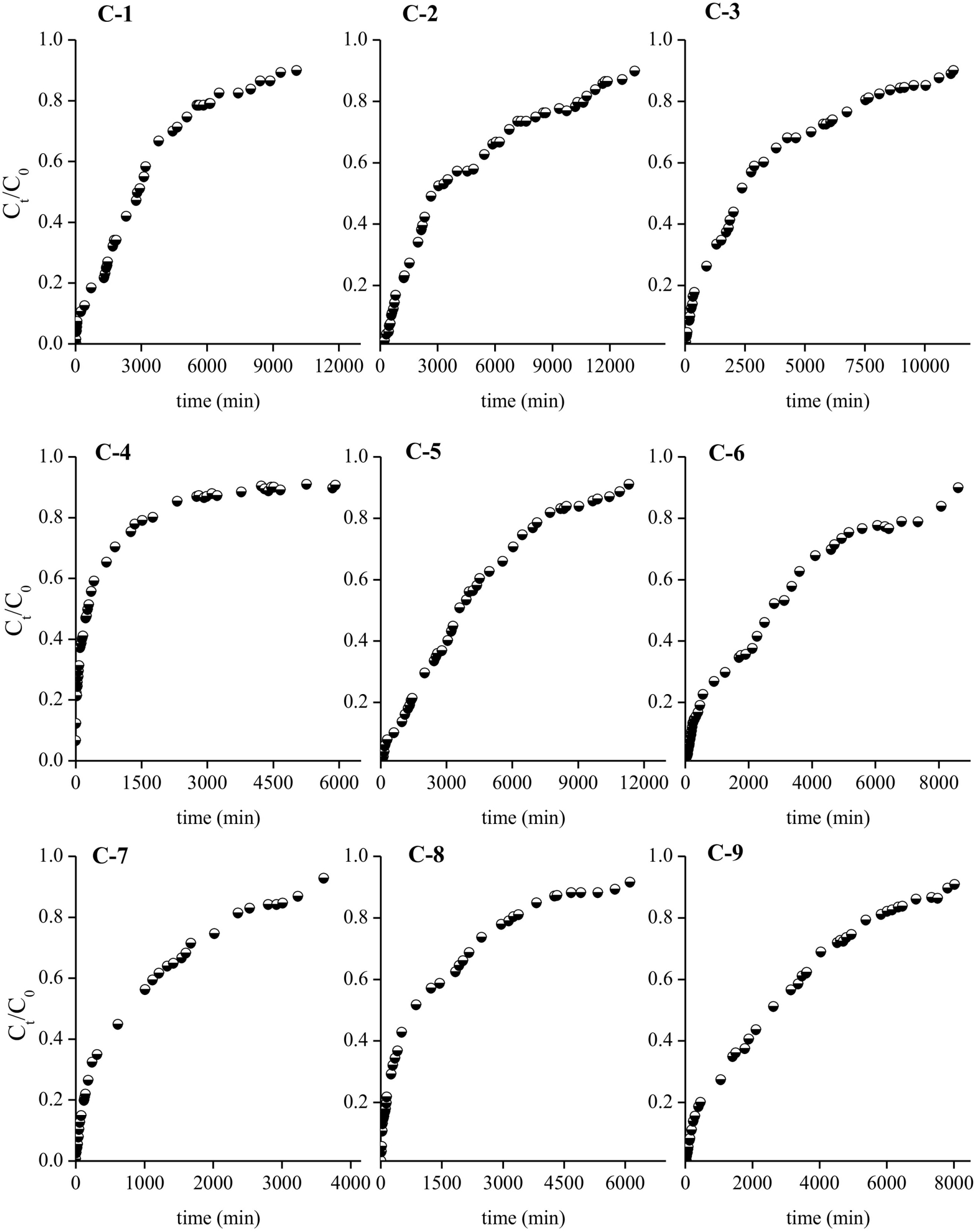
C-1
C-2
C-3
C-4
C-5
C-6
C-7
C-8
C-9
C_t/C_0
time (min)
0.0
0.2
0.4
0.6
0.8
1.0
0
3000
6000
9000
12000
2500
5000
7500
10000
1500
4500
2000
4000
8000
1000

Figure 7